

#### 4. Towards the Galactic Rotation Curve Beyond 12 kpc with ELODIE

A good knowledge of the outer rotation curve is interesting since it reflects the mass distribution of the Galaxy, and since it permits the kinematic distance determination of young disk objects. The rotation curve between 12 and 16 kpc is not clearly defined by the observations as can be seen on Figure 3. Both the gas data and the cepheid data clearly indicate a rotation velocity decrease from  $R_{\odot}$  to  $R=12$  kpc, but then the gas data outline a flat or rising curve at  $v_{\text{rot}} \approx 230 \text{ km s}^{-1}$  for  $R > 12$  kpc. The present cepheid sample suffers an effective cutoff in radial velocity measurements around  $V=12.5$  mag, so that the range in galactocentric distances that it covers is limited to the one indicated in the figure.

ELODIE is a high-resolution (45,000) fibre-fed spectrograph with a fixed wavelength range from 3900 to 6800 Å. It was built by collaboration between the Haute-Provence Observatory, the Marseilles Observatory and the Geneva

Observatory and is now permanently installed at the 1.93-m telescope of the Haute-Provence Observatory. This instrument possesses an automatic reduction programme called INTER-TACOS running on a SUN SPARC station to achieve on-line data reductions and cross-correlations in order to get the radial velocity of the target stars minutes after the observation. The cross-correlation algorithm used to find the radial velocity of stars mimics the CORAVEL process, using a numerical mask instead of a physical one (for any details, see Dubath et al. 1992). This technique allows us to extract easily the radial velocity of cool stars (later than F0) from spectra having a signal-to-noise ratio of about one and thus to get the velocity of Cepheids of 15<sup>th</sup> magnitude with an exposure time of about one hour or so (see Fig. 4).

We initiated last winter a programme of about 25 cepheids to cover the 11–15 kpc range of galactocentric distances. The approximate positions of the target cepheids are indicated as crossed hexagons on Figure 2. The analysis of this sample should constrain

the rotation curve from 12 kpc to 15 kpc and answer the question:

“Does the dip of the rotation curve at 11 kpc exist and does the rotation curve determined from cepheids follow the gas rotation curve?”

The answer will give an important clue about the reality of a local non-axisymmetric motions and will permit to investigate a possible systematic error in the gas or cepheids distance scale (due for instance to metal deficiency).

#### References

- Baranne A., Mayor M., Poncet J.L., 1979, *Vistas in Astronomy* **23**, 279.  
Blitz, L., Fich, M., Stark, A.A., 1982, *ApJS* **49**, 183.  
Clemens, D.P., 1985, *ApJ* **295**, 422.  
Dubath, P., Meylan, G., Mayor, M., 1992, *ApJ* **400**, 510.  
Feast M.W. & Walker A.R. 1987, *ARAA* **25**, 345.  
Fux, R., 1994, in preparation.  
Mermilliod J.-C., Mayor M., Burki G., 1987, *A&AS* **70**, 389.  
Pont F., Mayor M., Burki G., 1994a, *A&A* in press.  
Pont F., Mayor M., Burki G., 1994b, *A&AS* in press.

## Interstellar Na I Absorption Towards Stars in the Region of the IRAS Vela Shell

M. SRINIVASAN SAHU<sup>1,2</sup> and A. BLAAUW<sup>3</sup>

<sup>1</sup>Nordic Optical Telescope Group, La Palma, Spain; <sup>2</sup>Instituto de Astrofísica de Canarias, Tenerife, Spain;

<sup>3</sup>Kapteyn Laboratorium, Groningen, The Netherlands

### Introduction

The H $\alpha$  emission associated with the Gum Nebula is confined to a circular region which has a diameter of approximately 36° (Chanot and Sivan, 1983). In the southern brighter part of the nebula, near  $\gamma^2$  Velorum, the emission measure is higher by a factor of  $\sim 3$  as compared to the fainter, outer regions. We examined the IRAS SuperSky Flux maps in the entire Gum Nebula region and discovered a ring-like structure (Fig. 1) coincident with the bright southern part, which we have termed the IRAS Vela Shell (Srinivasan Sahu, 1992; Srinivasan Sahu and Blaauw, 1994). This structure, centred around the Vela OB2 group of stars (the B-association of which  $\gamma^2$  Velorum is a member, which we will refer to as Vela OB2, according to the nomenclature of Ruprecht et al., 1981), has an average radius of  $\sim 8^\circ$ . The section of the IRAS Vela Shell at

positive galactic latitudes is not clearly seen due to confusion with the background galactic emission. The half circle of dark clouds at negative latitudes coincident with the IRAS Vela Shell is apparent in the maps by Feitzinger and Stüwe (1986), in their study of the projected dark cloud distribution of the Milky Way. The IRAS maps clearly show that the cometary globules and dark clouds in the Puppis-Vela region, catalogued from the ESO-SERC IIIaJ plates (for example, Hawarden and Brand, 1976), are part of this ring-like structure.

The members (known and probable) of Vela OB2 lie within the IRAS Vela Shell which in fact just envelops the stars in this association. The Vela OB2 stars are therefore physically associated with the IRAS Vela Shell. Based on distance estimates to  $\gamma^2$  Velorum and Vela OB2, the distance to the centre of this

ring-like structure is  $\sim 450$  pc and its estimated mass is  $\sim 10^6 M_{\odot}$ . Both from the morphology on IRAS maps as well as from a study of the kinematics of the ionized gas in Puppis-Vela (Srinivasan Sahu and Sahu, 1993) the IRAS Vela Shell and the Gum Nebula appear to be two separate structures which just happen to overlap in projection.

We have analysed proper motions of the early-type stars in the region and there is strong evidence that the Vela OB2 stars are indeed part of a B-association. The association nature is further confirmed by the fact that both from position in the galactic (l, b) diagrams and its distance, Vela OB2 appears to form an extension of the string of association subgroups known as the Sco-Cen association and thereby a part of the Gould belt. Strömgren photometry by Eggen (1982) and an analysis by us using data from the homogeneous

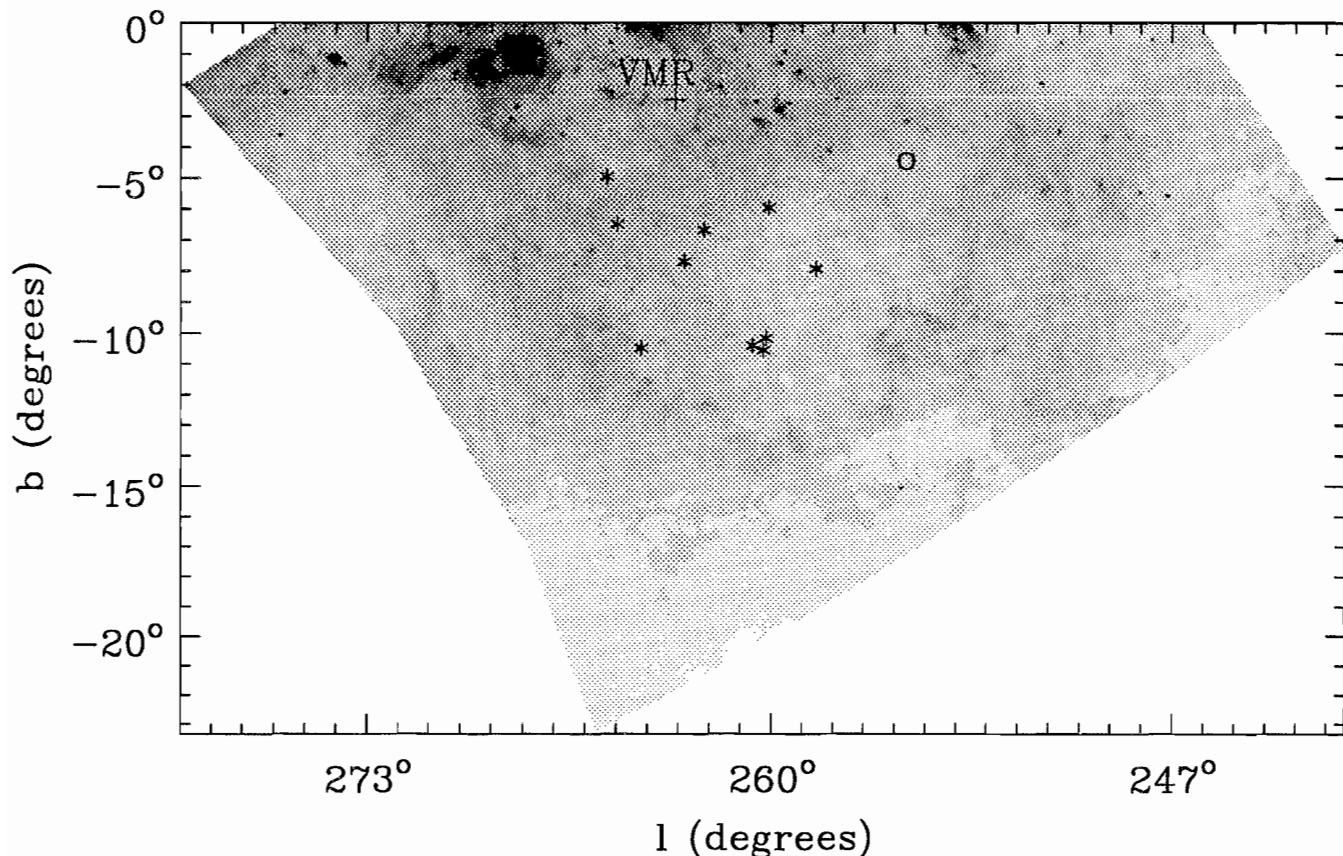


Figure 1: The IRAS Vela Shell at  $60 \mu\text{m}$ , obtained from the IRAS SuperSky Flux maps. The positions of the Vela OB2 stars are shown by "star" symbols,  $\zeta$  Puppis by an open square and the Vela pulsar by a plus sign.  $\zeta$  Puppis and the Vela pulsar are located near the edges of this shell, while the IRAS Vela Shell is clearly seen to envelop the Vela OB2 stars. This suggests that the Vela OB2 stars are physically associated with the shell and are the source of energy. The optically catalogued cometary globules and dark clouds in the Puppis-Vela region are part of the IRAS Vela Shell. The general location of the Vela Molecular Ridge (VMR) is also indicated in the plot.

ubvy-H $\beta$  catalogue of Hauck and Mermilliod (1991), indicates that this association is aged ( $\sim 2$  to  $3 \times 10^7$  years old) and on the verge of disintegration.

### Aim of the Study

The distribution and the kinematics of the NaI absorbing gas can help to understand this component of the interstellar medium in the IRAS Vela Shell. The Goddard High-Resolution Spectrograph (GHRS) on the Hubble Space Telescope with a resolving power of  $R \sim 80,000$  and wavelength range from  $1150 \text{ \AA}$  to  $3200 \text{ \AA}$ , has been used to study the properties of the highly ionized absorbing gas in each individual component for the case of  $\gamma^2$  Velorum (Fitzpatrick and Spitzer, 1993). However, there are no good-quality optical data with comparable resolution which can be combined with the GHRS data to study the weakly ionized and neutral components in the IRAS Vela Shell. For these reasons, in January 1993, we initi-

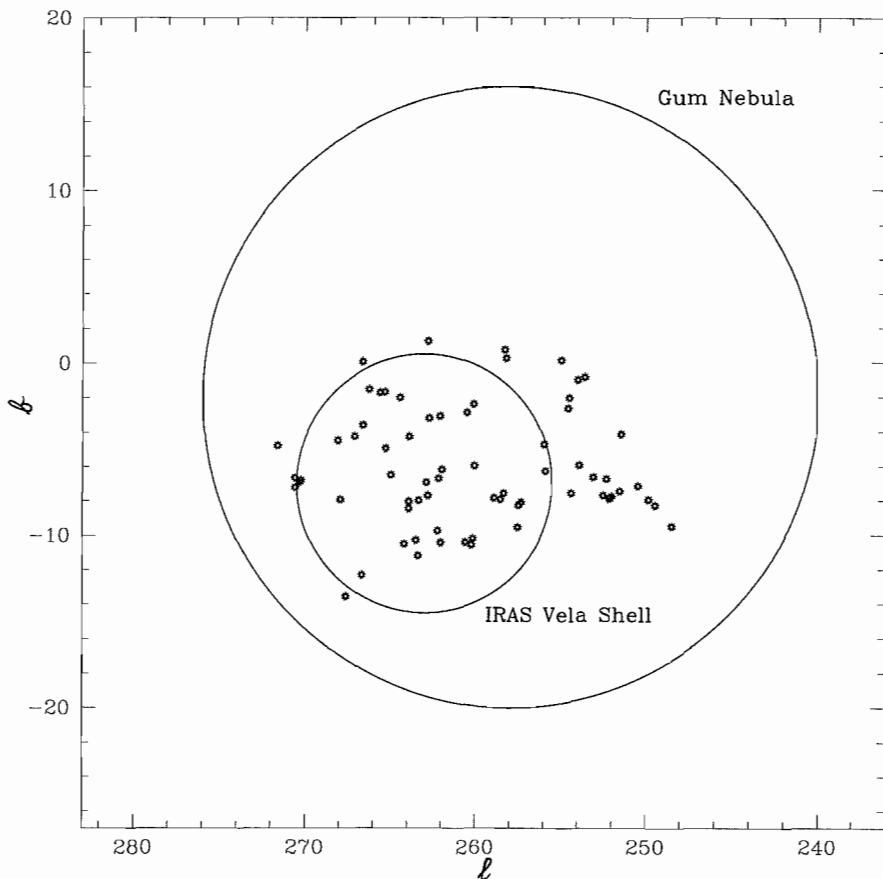


Figure 2: Schematic figure showing the locations of the IRAS Vela Shell, the Gum Nebula and the stars that we have observed.

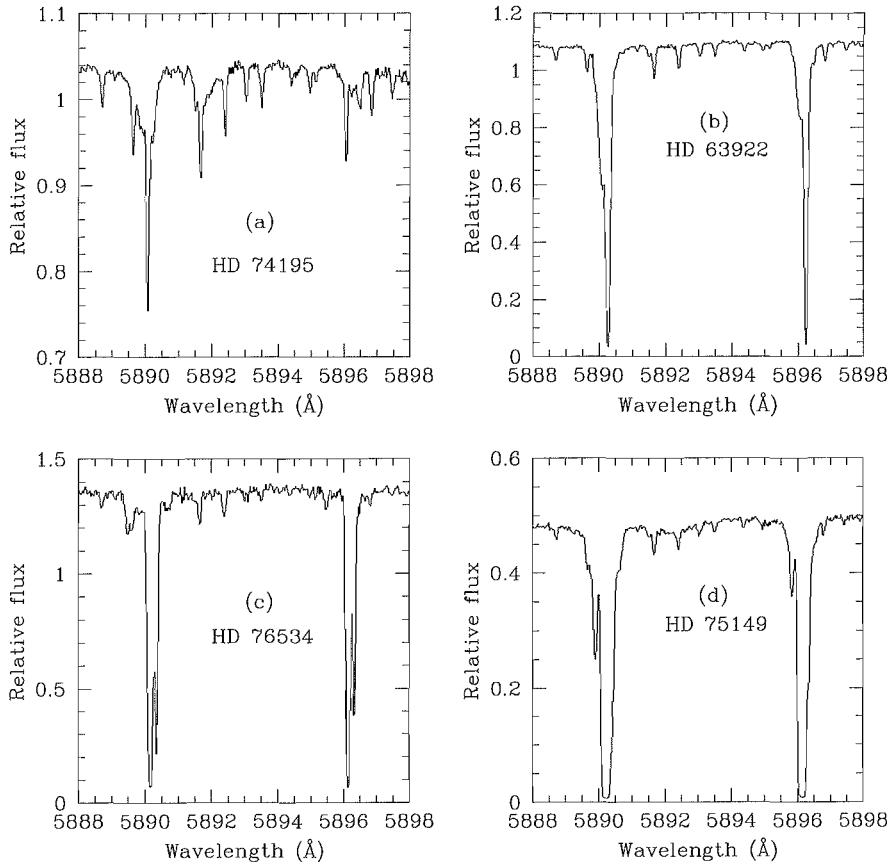


Figure 3 (a–d): The Na I  $D_1$  and  $D_2$  region in the spectra of four stars in our sample: (a) HD 74195, a member of the cluster IC 2391 which is at a distance of  $\sim 170$  pc (b) HD 63922, a member of Vela OB2, located at  $\sim 450$  pc (c) HD 76534, a member of Vela R2, located at  $\sim 700$  pc and (d) HD 75149, a member of Vela OB1 (Humphreys, 1978) located at  $\sim 1500$  pc. Note that the spectra have not been corrected for the influence of telluric lines.

ated a high-resolution ( $R \sim 80,000$ ) study of the Na I  $D_1$  and  $D_2$  absorption lines in the line of sight to stars in the region of the IRAS Vela Shell.

Our sample consists of  $\sim 75$  early-type stars (spectral types O9 to B7) whose locations with respect to the IRAS Vela Shell and the Gum Nebula are shown in Figure 2. The distances to these stars were determined using published spectroscopic/photometric data as well as proper motion data obtained from the Hipparcos Input Catalogue. There is fairly good agreement between the values of the distances obtained by these two methods for the case of relatively nearby stars. The distances for the stars in our sample range from  $\sim 150$  to 2000 pc and galactic altitudes ( $|z|$ ) range up to  $\sim 160$  pc.

### Observations and Future Prospects

We have obtained fairly high S/N ( $\sim 60$  to 500) Na  $D_1$  and  $D_2$  spectra for all the stars in our sample. The 1.4-m Coudé Auxiliary Telescope (CAT) and the Coudé Echelle Spectrograph (CES) in combination with the Long Camera

and the UV-coated Ford Aerospace/Loral 2048 $\times$ 2048 CCD (#27) was used for all our observations. This CCD has a pixel size of  $15 \mu\text{m} \times 15 \mu\text{m}$ , a low dark current ( $3 \text{ e}^-/\text{pixel}/\text{hour}$ ), a low readout noise ( $\sim 6 \text{ e}^-$  rms) and appears to have few defects. The net efficiency of this system is: 3.8 % at 5400 Å and 4.6 % at 6450 Å (Pasquini et al., 1992). We have used this instrument configuration both at La Silla and by means of remote control from Garching, with satisfactory results.

We have used MIDAS for our data reduction. After the standard bias and background subtractions and flat fielding procedures, we extracted orders by using only the central 4 to 6 columns which had the highest S/N ratios, in the stellar and thorium lamp frames. This was done to avoid the contribution due to background scattered light. We opted to use a weighted average (weighted according to their S/N ratio values) of these central 4 to 6 columns rather than a simple average since the S/N ratios for the case of the weighted average method was typically higher than the simple average method by a factor  $\sim 1.5$  to 2. Thus, normalized two-dimensional

spectra were obtained for stars and the thorium lamp. The stellar spectra were wavelength calibrated by using the thorium spectra taken either preceding or following the stellar exposure. We identified typically 30 to 35 lines in the thorium spectra with the help of the Atlas of the Thorium-Argon Spectrum (D’Odorico et al., 1987) and fitted polynomials to obtain relationships between the wavelength and pixel number. The polynomial fits had residuals with an rms scatter of  $< 0.0045 \text{ \AA}$  for all the spectra. Figure 3 (a–d) shows the Na I  $D_1$  and  $D_2$  region in the spectra of four of the stars in our sample.

The Na I  $D_1$  and  $D_2$  lines fall in a spectral region which has numerous telluric lines mostly due to atmospheric water vapour. The strengths of the telluric lines caused by water vapour can vary by a factor of two or more within a matter of a few hours, even at a high altitude observatory like La Silla (A. Ardeberg, private communication). Therefore, the telluric lines contaminate the information present in the spectra and they can cause serious problems, particularly in the case of the faint components. We are now in the process of correcting the stellar spectra for the influence of the telluric lines using the synthetic telluric spectrum in the region of the  $D_1$  and  $D_2$  lines, constructed by Lundström et al. (1991).

We intend to pursue this observational programme and observe the Ca II absorption in the line of sight to our sample stars, to obtain Na I/Ca II ratios, whenever possible for each component. The Na I/Ca II ratio traces changes in the calcium abundance in the absorbing gas. Calcium is released in the gaseous phase when grain destruction occurs due to violent events such as, for example, supernovae. Therefore, in addition to determining the distribution and kinematics of the absorbing gas, we expect to learn more about the history of the IRAS Vela Shell through these observations.

### References

- Chanot, A., Sivan, J.P.: 1983, *Astron. Astrophys.* **121**, 19.
- D’Odorico, S., Ghigo, M., Ponz, D.: 1987, ESO Scientific Report No. 6.
- Eggen, O.J.: 1982, *Astrophys. J. Suppl. Ser.* **50**, 199.
- Feitzinger, J.V., Stüwe, J.A.: 1984, *Astron. Astrophys. Suppl. Ser.* **58**, 365.
- Fitzpatrick, E.L., Spitzer, L.: 1993, Princeton Observatory Preprint No. 541.
- Hauck, B., Mermilliod, M.: 1991, obtained through the SIMBAD data retrieval facility.
- Hawarden, T.G. and Brand, P.W.J.L.: 1976, *Monthly Notices Roy. Astron. Soc.* **175**, 19P.

Humphreys, R.M.: 1978, *Astrophys. J. Suppl.* **38**, 309.  
 Lundström, I., Ardeberg, A., Maurice, E., Lindgren, H.: 1991, *Astron. Astrophys. Suppl. Ser.* **91**, 199.

Ruprecht, J., Balazs, B., White, R.E.: 1981, *Catalogue of Star Clusters and Associations*, Supplement I, Part B2, ed. B. Balazs (Akademiai Kiado, Budapest), p. 471.  
 Srinivasan Sahu, M.: 1992, Ph. D. thesis,

University of Groningen.  
 Srinivasan Sahu, M. and Blaauw, A.: 1994, *Astron. Astrophys. Main Journal* (subm.).  
 Srinivasan Sahu, M. and Sahu, K.C.: 1993, *Astron. Astrophys.* **280**, 231.

# A Radial Velocity Search for Extra-Solar Planets Using an Iodine Gas Absorption Cell at the CAT + CES

M. KÜRSTER<sup>1</sup>, A.P. HATZES<sup>2</sup>, W.D. COCHRAN<sup>2</sup>, C.E. PULLIAM<sup>2</sup>, K. DENNERL<sup>1</sup>  
 and S. DÖBEREINER<sup>1</sup>

<sup>1</sup>Max-Planck-Institut für Extraterrestrische Physik, Garching, Germany

<sup>2</sup>McDonald Observatory, The University of Texas at Austin, Austin, U.S.A.

## Introduction

The origin of the solar system is a fundamental problem in astrophysics for which many basic questions remain to be answered. Is planet formation a common or rare phenomenon? Is it a natural extension of the star formation process or is a different mechanism involved? Unlike most stars, the Sun is not found in a binary system. Is its single status related to the fact that it has a planetary system? Unfortunately, the answers to these and other important questions are hampered by the fact that the only known example of a planetary system (around a non-degenerate star) is the one around the Sun. Clearly, before one can develop general theories of planet formation, one must collect a large body of astronomical data that includes the frequency of planetary systems, the planetary mass function, and the correlation of such systems with mass, age, stellar composition, etc. of the primary star.

Although a number of direct and indirect techniques have been proposed for extra-solar planet detections, radial velocity measurements are proving to be a cost effective means of using ground-based facilities to search for planets. What radial velocity precision is needed to detect Jovian-sized planets? Naturally, one uses the Jupiter-Sun system as a guide where the Sun orbits around the barycentre with an average velocity of  $12 \text{ m s}^{-1}$  and a period of 12 years. Thus, an instrument capable of measuring relative stellar radial velocities to a precision better than  $10 \text{ m s}^{-1}$  and with a decade-long stability should be able to detect the presence of a Jovian-massed planet orbiting 5 AU from a solar-type star. Lower mass objects can be detected in orbits with smaller semi-major axes.

## Radial Velocity Technique

Traditional radial velocity measurement techniques rarely exceed a precision of  $200\text{--}500 \text{ m s}^{-1}$ . The reason for this is that the wavelength reference is taken at a different time and often traverses a different light path than that of the stellar spectrum. Use of radial velocity standard stars circumvents the problem of different light paths for the reference and stellar spectra, but the standard observation is still made at a different time and there is always the danger that the standard star is a low-amplitude variable.

The instrumental errors can be

minimized by superimposing the wavelength reference on top of the stellar observation. One means of accomplishing this is to pass the starlight through an absorbing gas prior to its entrance into the spectrograph. The gas produces its own set of absorption lines against which velocity shifts of the stellar spectrum are measured. Since instrumental shifts now affect both the wavelength reference and stellar spectrum equally, a high degree of precision is achieved.

Griffin and Griffin (1973) first proposed using telluric  $\text{O}_2$  lines at  $6300 \text{ \AA}$  as a radial velocity reference. In this

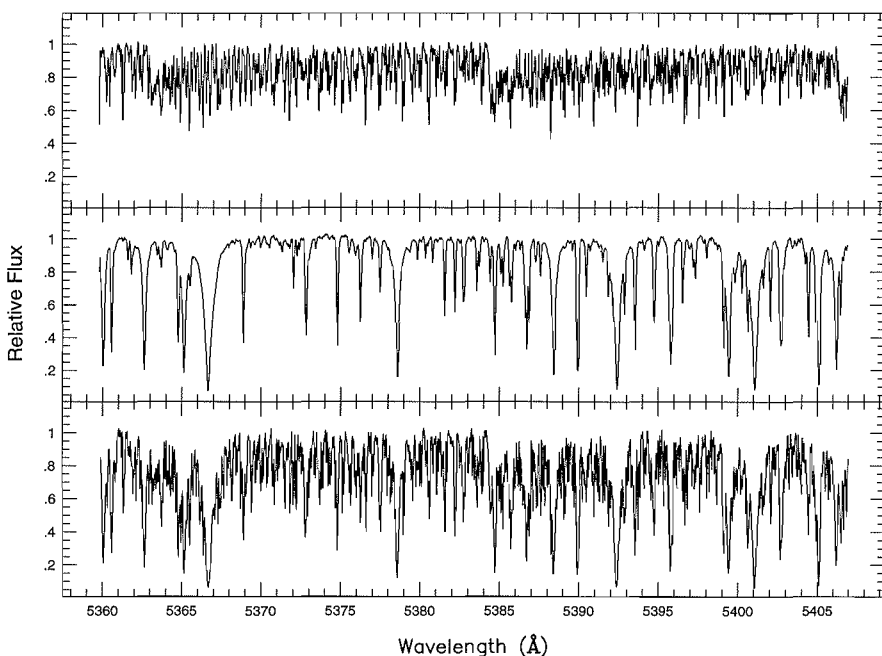


Figure 1: (Top) Absorption spectrum of the  $\text{I}_2$  cell obtained by taking a dome flatfield through the cell. (Middle) Spectrum of  $\alpha \text{ Cen B}$  without the  $\text{I}_2$  cell from  $5360 \text{ \AA}$  to  $5407 \text{ \AA}$ . (Bottom) Spectrum of  $\alpha \text{ Cen B}$  taken with the  $\text{I}_2$  cell in front of the entrance slit of the ESO CES. All spectra have been normalized to the continuum.